Stirred tanks: A Physical Explanation for the Exponents of Classical Empirical Mass Transfer Equations

Mariano Martín, Francisco J. Montes, Miguel A. Galán.

Universidad de Salamanca, Departamento Ingeniería Química y Textil, Plaza de los Caídos, 1-5, 37008 Salamanca (Spain), Telf: 00 34 923 294479; Fax: 00 34 923 294574
mariano.m3@usal.es; javimon@usal.es; magalan@usal.es

Abstract.

In order to illuminate the effect of the scale on the oxygen transfer in stirred tank reactors, a combined study of the hydrodynamics and the mass transfer has been carried out. The air water system was used to study the behaviour of different impellers against the gas phase and its result in the volumetric mass transfer coefficient. The correct prediction of the rate of oxygen transfer by means of a theoretical basis has also been achieved based on the typical theories of mass transfer, and the study of the hydrodynamics of the system.

Introduction.

Biochemical productions, transformation and degradation of chemical compounds have become major operations in the chemical process industries. Production of proteins, enzymes, vitamins, pharmaceutical compounds and degradation of heavy metals, pesticides, petroleum based compounds and water wastes are very good known processes.

Most of these processes take place in stirred tank reactors where the purpose of aeration is to transfer oxygen from air bubbles generated in pipes or sieve plates into the liquid phase where the biological reactions occur. The base for its design has traditionally been the empirical correlations obtained for different scales, often lower than the industrial scale. Scale up has become the major problem due to the wide variety of results obtained.

The central point of the mass transfer process is the contact between phases. This fact is related to the dispersion of the gas phase in the liquid phase due the dispersion device and to the effect of the impeller on the bubbles.

In this work the study of the hydrodynamics generated by different impellers and dispersion devices in a non standard tank will allow a better understanding of the generation of gas dispersions. The parallel determination of the volumetric mass transfer coefficient for all the configurations whose hydrodynamics is studied will make possible to explain the experimental results. Apart from the direct explanation, theoretical equations were developed and used to predict the volumetric mass transfer coefficient from the hydrodynamic results.

Experimental methods and set up.

The experimental set up can be seen in Figure 1. The set up consists of an optical table on which the other devices are fixed. Bubbles are generated in a bubble column, which is aligned with a high speed video camera, Redlake Motionscope®, capable of recording up to 1000 frames per second. The system is illuminated by an optic fibre device which allows the control of the light intensity and its distribution. Images recorded are edited and analysed by means of MOTIONSCOPE® software.
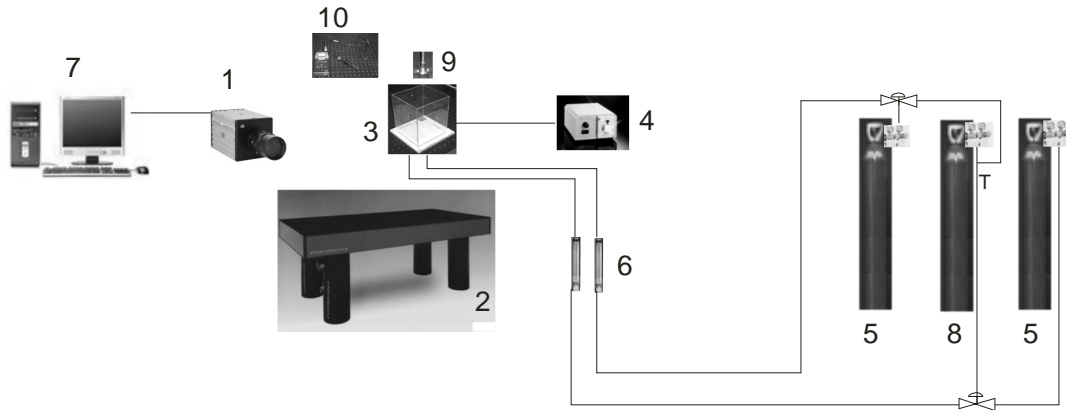
Figure 1.-Experimental set up. 1.-High speed video camera; 2.-Optic table; 3.-Bubble column; 4.-Illumination source; 5.-Air compressed; 6.-Rotameters; 7.-Computer; 8.-Nitrogen; 9.-Impeller; 10.- Oxygen electrode

Fixed to the bottom of the bubble column, a gas chamber divided in two was used to feed air separately. Different dispersion devices, one and two holed sieve plates, which are the exits of the two gas chambers, and five impellers were used so that a certain level of generality can be achieved. Apart from the typical Ruston turbine, two pitched blade turbines, the propeller and a modified blade were tested varying the gas flow rate, the rotation speed and their relative position to the dispersion device along the vertical axis.

For all of these conditions the dispersions generated were recorded, its hydrodynamics simulated using a commercial CFD code (CFX 5.7 based on ANSYS 8.1) and the volumetric mass transfer coefficient measured, by means of the dynamic method using an oxygen electrode

Theoretical background.

The mass transfer film resistance depends on the contact time, which, at the same time, is related to the hydrodynamics, to the mixing in the tank. Two scales of mixing determine the degree of mixing in the tank, the macromixing, responsible for the homogenization of the liquid in the tank and subject to the scale up problems, and the micromixing, due to the turbulent eddies generated and the predominant mechanism in case of chemical reaction [1,2]. This fact, along with the Higbie's theory [3] eq. (1),

$$k_L a = k_L \cdot a = \sqrt{\frac{4 \cdot D_L}{\pi \cdot t}} a \tag{1}$$

and the study of the breakup effectiveness of the combination between the impeller and the dispersion device in order to provide specific area using empirical equations related to the power input somehow based on the Kolmogorov's theory [4], developed from eq. (2) [5] were the basis for the theoretical equation.

$$a = 1.44 \left[\frac{\left(\frac{P_g}{V} \right)^{0.4} \cdot \rho^{0.2}}{\sigma^{0.6}} \right] \left(\frac{u_G}{U_\infty} \right)^{0.5} \tag{2}$$

The combination of both concepts and the definitions of mixing time eq.(3) [6]

$$\theta = 5.9 \cdot \left(\frac{T}{D}\right)^{-1/3} \cdot \varepsilon^{-1/3} \cdot D^{2/3} \tag{3}$$

or the micromixing time and the correlations to modify the power input due to the gas phase, eq. (4)

$$P_g = C' \cdot P \cdot We^m \cdot N_A^{\gamma} \cdot (\rho_L/\rho_D)^n = C' \cdot P \cdot \left(\frac{N^2 T^3 \rho_L}{\sigma}\right)^m \cdot \left(\frac{u_G \cdot \pi \cdot (D/2)^2}{N \cdot T^3}\right)^{\gamma} \cdot (\rho_L/\rho_D)^n \tag{4}$$

allowed the development of equations like eq. (5) able to explain and predict the coefficients of the typical empirical equations eq. (6)

$$k_L a = C' \cdot \frac{D_L^{0.5} \cdot \rho^{1/30+0.4\chi}}{\sigma^{0.6+0.2\chi}} \cdot \left(\frac{\mu_W}{\mu_{app}}\right)^{0.25} \cdot \frac{T^{1/6}}{D^{0.5}} \cdot \left(\frac{\sigma}{N^2 T^3 \rho_L}\right)^{m/6} \cdot \left(\frac{N \cdot T^3}{D^2}\right)^{\gamma/6} \cdot \left[\left(\frac{P_g}{V}\right)^{(1/6)+\delta-\delta\chi/2}\right] (u_G)^{\chi-\gamma/6} \tag{5}$$

$$k_L a = k \cdot \left(\frac{P_g}{V}\right)^{\alpha} \cdot u_G^{\beta} \tag{6}$$

Results and discussion.

The hydrodynamics

N= 180rpm; Q_e=0,6·10⁻⁴m³/s   N=180rpm; Q_e= 1,4·10⁻⁴m³/s   N= 180rpm; Q_e=2,8·10⁻⁴m³/s

N=280rpm; Q_e= 0,6·10⁻⁴m³/s   N= 280rpm; Q_e=1,4·10⁻⁴m³/s   N=280rpm; Q_e= 2,8·10⁻⁴m³/s

N=430rpm; Q_e= 0,6·10⁻⁴m³/s   N= 430rpm; Q_e=1,4·10⁻⁴m³/s   N= 430rpm; Q_e=2,8·10⁻⁴m³/s
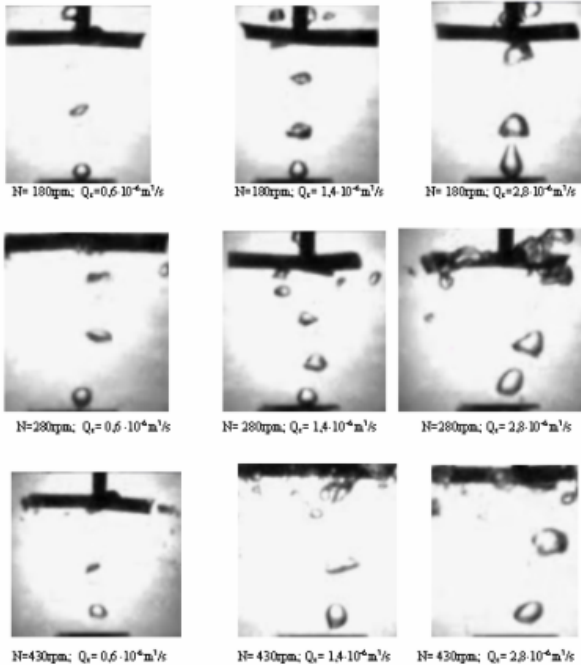
Figure 2.- Rising path of the bubbles under mixing conditions

The study of the hydrodynamics inside the stirred tank was carried out using CFD, to determine the power number in each of the configurations, and high speed video techniques.

The hydrodynamics of the dispersions generated was characterised by the sauter mean diameter of the dispersion, responsible for the specific area of the bubbles as well as by the recorded dispersion itself, and the characteristics of the generated bubbles (formation time and period and bubble initial size).

In general, bubble initial size decreases with the rotational speed as well as its formation time and period. Bubbles can be swept from the orifices. The path the bubbles describe in their rising depends on the impeller and is responsible for the direct effect of the impeller on the bubbles, Fig. 2.

The initial size of the bubbles determined the break up process and so the sauter mean diameter of the dispersion. The particular flow pattern developed by each of the impellers defined the disposition of the bubbles across the reactor.

The sauter mean diameter and its relationship with the power input can be correlated to equations of the form:

$$d_{32} = k_d \cdot \left(\frac{P_g}{V}\right)^{\delta}$$

(7)

The results for the five types of impellers reveal that for big bubbles, those generated at the one holed sieve plate, δ was bigger, in absolute terms, and in case the impellers are capable of breaking the bubbles, like the pitched blade turbine and the Rushton turbine, δ was similar to that proposed by Kolmogorov, -0,4 meanwhile for smaller initial bubbles, impellers were not able to break the bubbles easy and the δ coefficient goes from -0,04 to -0,25

The mass transfer rate.

The exponent related to the power input per unit volume in eq. (6), (α), turned out to depend on the break up of the bubbles as well as on the quality of the dispersion, the specific area available and the atmospheric contribution due to the turbulence generated at the liquid – gas surface which replace the surface of the liquid.

The exponent related to the superficial gas velocity in eq. (6), (β), depended on the effect of the gas on the impeller and on the specific area available of the dispersion.

With the experimental results of the hydrodynamics for the five impellers, the δ coefficient, and the effect of the gas flow rate on the superficial area, the experimental coefficients α and β determined by the dynamic method can be predicted using the theoretical equations. Good agreement was obtained.

In both cases, with a dispersion of bubbles experimentally obtained in a tank [7], it is possible to determine, using the developed equations, the pattern of each of this coefficients throughout the tank. Figure 4 represents these patterns. The most favourable region of the tank for the mass transfer process is next to the impeller where the contact area is high due to the break up of the bubbles.

Neither α nor β depended on the scale of the tank [8 - 13]. However, the constant k gathered the influence of the physical properties of the liquid, the influence of the transport properties and the atmospheric contribution due to the position of the impellers and what is more important, the influence of the predominant flow scale in the tank.
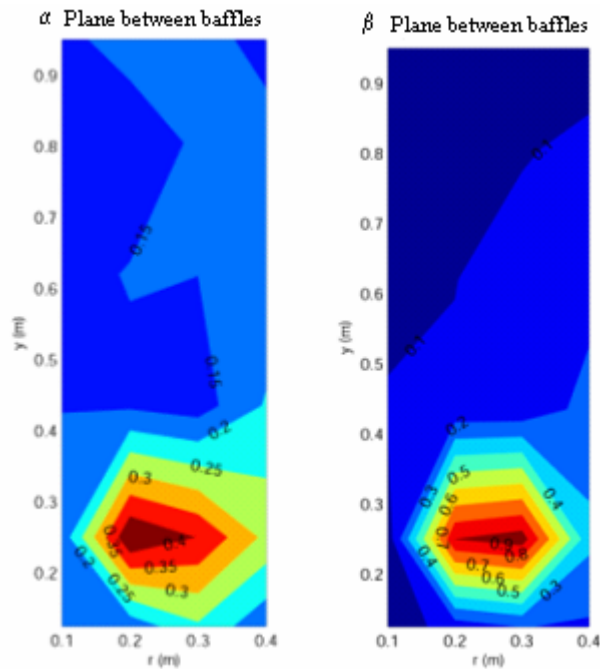
Figure 4.- α and β pattern across the tank

It was proved that, in absence of consumption of oxygen in the tank, the volumetric mass transfer coefficient, $k_L a$, can be predicted as a combination from that obtained considering the contact time given by the mixing time and by that given by the micromixing. An equation was proposed to weight up both behaviours since the presence of gas phase conditioned the mixing.
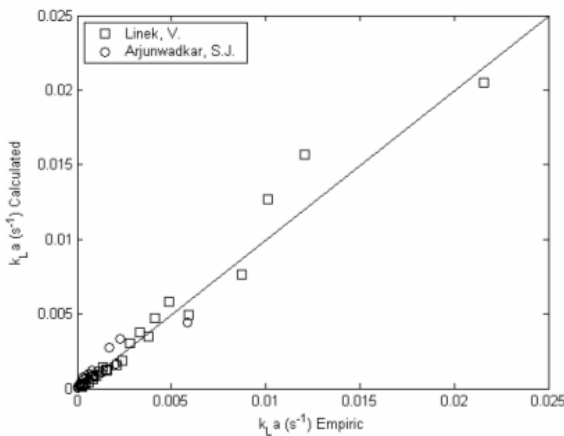

Figure 5.- Fitting of the volumetric mass transfer coefficient to the equation (8)

$$k_L a = \frac{1}{f_M} \left(k_L a_{Micromixing} \left(1 - \varepsilon_g \right) + k_L a_{Macromixing} \cdot \varepsilon_g \right)$$

(8)

Good agreement was found, figure 5. f_M is related to the different geometries and impellers used for the authors [14, 15]. In case of oxygen consumption, the enhancement allows to almost predict the $k_L a$ by means of that proposed by the micromixing hiding the macromixing effects.

Nomenclature.

d_{32}: Sauter mean diameter (m)
D: Tank diameter (m)
D_L: Diffusivity (m^2·s)
f_M: Geometry factor.

k: Constants

k_La : Volumetric mass transfer coefficient (m·s^{-1})

g: Gravity (m·s^{-2})

m: Aeration coefficient related to We.

n: Aeration coefficient related to densities..

N: Rotacional speed (s^{-1})

N_A: Aeration number $N_A = \dfrac{Q_c}{N \cdot T^3}$

N_p: Power number.

P: Unaerated agitation power (W)

P_g : Aerated input power (W)

Q_c: Gas flow rate (m^3·s^{-1})

Re: Reynolds number. $Re = \dfrac{T^2 N \rho}{\mu}$

Sc: Schmidt number $Sc = \dfrac{\mu}{\rho \cdot D_{ab}}$

T: Impeller diameter (m)

u_G: Superficial gas velocity (m·s^{-1})

U_B: Rising velocity (m·s^{-1})

V: Tank volume (m^3)

w: Velocity at the end of the blade (m·s^{-1})

We: Weber number $We = \dfrac{\rho N^2 T^3}{\sigma}$; $We_{Bubble} = \dfrac{d_{eq} \cdot U_B^2 \cdot \rho}{\sigma}$

α y β : Empirical coefficient

δ: Empirical coefficient related to bubble diameter.

γ: Empirical coefficient related to the aerated input power

ε: Gas hold up.

ε_i: Energy per unit mass.

μ: Viscosity (Pa·s)

ρ: Liquid density (kg·m^{-3})

θ : Mixing time (s)

σ: Surface tension (N/m)

Subindexes.

L: Liquid

D: Dispersion

References

[1] Baldyga, J. ; et al (1997), Chem. Eng. Sci., 52, 4, 457-466

[2] Zlokamik, M. (2002) Wiley VCH, Weinheim

[3] Higbie, R., (1935) , Trans. Am. Ins. Chem. Eng., 31, 365–389.

[4] Kolmogorov, A.N. (1949). Dokl. Akad. Nauk. SSSR 66, 825-828

[5] Calderbank, P.H. (1958), Trans Inst. Chem. Eng, 36, 443-463

[6] Nienow, A.W. (1997) Chem. Eng. Sci., 52, 15, 2557-2565

[7] Barigou, M.; et al Chem. Eng. Sci., 47, 8, 2009-2025

[8] Ózbek, B.; et al (2001) Process Biochemistry, 36, 729-741

[9] Wu, H. (1995) Chem. Eng. Sci., 50, 17, 2801-2811.

[10] Puthli, M.S.; et al (2005) Biochemical Engineering Journal, 23, 25-30

[11] Gogate, P.R., (2001) et al., Bioch. Eng. J., 6, 109-144

[12] Montes, F.J. PhD Thesis (1996) University of Salamanca, Spain

[13] Sanchez, J.M, PhD Thesis. (2003) University of Salamanca, Spain

[14] Arjunwadkar, S. J.; Sarvanan, K.; Pandit A.B.; Kulkarni P.R (1998) Biochem. Eng. J., 1, 25-30

[15] Linek, V.; Vacek.; Benes, P.; (1987) Chem. Eng. J., 34, 11- 34